DOI: https://doi.org/10.5281/zenodo.23270338



Purposeful scientific research as a pillar of sustainable development



New Software for Calculating Magnetic Flux Density in Magnetic Electron Lenses

R.Y. J. Al-Salih[1], E. M. A. Alkattan[2], A. I. M. Alabdullah[3]

[1] *Department of Physic, College of Science, Tikrit University, Iraq*

[2] *The General Directorate for Education in Nineveh Conservative, Iraq*

[3] *Department of Physics, College of Sciences, Mosul University, Iraq*

Email: r.y.jasim@tu.edu.iq

ABSTRACT

A new program has been written here to calculate magnetic flux line trajectories in magnetic electron lenses for axially symmetric and asymmetric magnetic systems, such as the magnetic electron lenses that are excited using coil windings. The recently introduced program used the acronym "CMFD" for "Calculating Magnetic Flux Density(MFD)". This program possesses many features, such as the flexibility of reading the input data using any text editor, the flexibility of exporting data to Microsoft Excel or Text File Extension, the ability to plot the magnetic flux lines directly, and the system circuit furthermore flexibly to change both of course and the fine meshes for finite element (FE) calculations. A new suggested design of magnetic lens has been investigated using this new software written in this work to demonstrate a part of the program's capabilities of studying the geometrical parameters effect of magnetic systems on the flux lines distributions. This study found that this new program is easy to use and can draw magnetic flux line trajectories with high clarity and accuracy.

Keywords: Electron Lens, Finite Element, Magnetic Flux Lines, Magnetic Lens Design

Introduction

The growth of Electron Optics initializes electron microscopes. Busch investigated the paths of charged-particles in electric and magnetic fields of axially symmetric systems (In 1926) [1]. He sets the basic groundwork of electron optics geometrical schemes and establishes that magnetic and electric fields could be optical lenses. On the same date, de Broglie produced the electron waves principle. It is commonly known that the charged particles were physically linked to a wavelength or frequency. This finding marked the start of the field of electron optics. These two innovations create the notion of the electron lens [2]. The electron lens is essential to electron microscopy and is considered vital to all such instruments [3]. Some defects in electron lenses arise during industrial processes; for example, "aberrations" that the lens construction is unable to concentrate all the rays that are produced from each point of the "object's plane" hooked on the corresponding point in the "image Gaussian plane" [4]. Then, it is necessary to control the trajectory with an appropriate appliance; otherwise, numerous lenses are needed until the proposed lens's interesting characteristics are achieved, which involves much exertion and expenses. The proper tools to resolve these problems are the simulators, mathematical models, and software packages used under the so-called "Computer-Aided Design (CAD) appliances". CAD of such optical assemblies often profits through three stages. The first stage is calculating magnetic or electric fields using boundary conditions. However, the second stage estimates the paths of the electrons by computing magnetic fields. The last stage is

DOI: https://doi.org/10.5281/zenodo.23270338

determining aberration values and imaging characteristics from estimated trajectories, The appliances employed for electromagnetic and electrostatic lenses are software programs to support operators in asymmetric and symmetric lenses of "single, double, and multi-polepiece lenses" utilized in electron microscopes. CAD is an influential appliance to aid researchers in examining many altered designs deprived of the need to manufacture suggested designs [5].

Literature Review

In earlier literature, many categories of software package sets besides simulators have been recycled; for example, SPOC software [6], G-Optk simulation software (SS) [7], EOD program [8], CPO programs [9], Focus software, SIMION software [10,11], EOS Simulator [12], MEBS software [13], Omni Trak software [14]. Workers should select a proper mathematical model amongst the obtainable models, such as Glaser model [15], Grivet Lenz model [16], Gaussian model [16], Spherical model [17], Exponential model [17]. Another advantage of software appliances is the typical shorthand in time, which is essential for the operators of SS to reduce both efforts and costs [18]. Hasan *et al.* (2013) wrote a new software specialized for magnetic lenses, called "CADTEL," which can be operated with PC systems [19]. Many various ideas have been trusted regarding the analysis methods in the twentieth century, like the effect of the saturation of pole-piece on focal features of objective lenses [20], and the influence of axial magnetic field distribution on the objective lenses that operate under high voltage electron microscopes [21]. The 1st one is termed "examination/analysis methodology", which is related to the investigation that consists of three categories named "H1 programs" for magnetic scalar potential by using circumstances of Laplace [22], in addition to "H2 & H3 programs" for magnetic vector potential by solving circumstances of Poisson [23]. The second one is "H4 programs" for "union/synthesis method". Scientists frequently used "Visual Basic language" for writing the suggested programs. Kadhem *et al.* (2018) have used FEM with the assistance of Munro packages to investigate asymmetrical magnetic lenses by combining "Electron Optical Design (EOD)" software [24]. Whereas Van Tilborg *et al.* (2018) employed "MHD simulations" for carrying out tests, they revealed the advantage of discharge capillaries of dynamic plasma lenses to focus 100 MeV of rays [25]. However, Shiltsev *et al.* (2109) rewrote "FMA & DA plots" for the demonstrative occurrence of "7 TeV protons" flux deprived of impacting the focused optics presentations [26]. Alabdullah *et al.* (2019) presented an improved design, termed "Focal Length Measurement (FLM)" that could examine electrostatic lens characteristics with analytical test processes. The newfangled FLM technique has been examined by computing focal lengths of the "electrostatic immersion lenses" [27]. Liu J. *et al.* (2020) described a simulation for the spatial resolution of a dilation imager built on the Monte Carlo method. The path of the electron is simulated, where the electron spot on the microchannel plate (MCP) is achieved. They found that the dilation imager uses a long magnetic focusing lens to image electrons from PC against the MCP with the image ratio of 2:1. The electron path is simulated, and the electron spot on the MCP is obtained. So, they found that the altitudinal resolution can be achieved from the electron distribution alongside the X-axis and the Y-axis on the MCP. The simulation consequences indicated that the image rotation angle of a long magnetic lens is 0°[28]. Liu J. *et al.* do another work in the same year (2020) simulated a short magnetic lens using Monte Carlo method and found that the width of the electron beam is enlarged while the electron beam moves in the drift region between mesh and MCP, and the dilated electron beam is captured by the MCP based framing camera [29]. Khan S. A. and Jagannathan R. (2021) had a well-thought-out scalar theory of quantum mechanics of electron optics at the single-particle level, resulting from the Dirac equation via a Foldy–Foldy-Wouthuysen-like transformation technique. Directed by the Ehrenfest theorem, quantum averages of locus and momentum of an electron beam in a plane crosswise to the optic axis of an electron optical system have been specified with classical ray coordinates.

DOI: https://doi.org/10.5281/zenodo.23270338

Round electromagnetic lenses with Glaser and power law models for axial magnetic field had been investigated particularly. They discovered that the quantum average position in the paraxial estimation complies with the Equation for classical paraxial motion [30]. AL-Janan and AL-Salih (2023) have found that magnetic flux density decreases when the diameter of the inner bore reduces, and both spherical and chromatic aberration factors decrease, leading to the improvement of all-optical characteristics, obtaining maximum flux density [31]. Fox J. *et al.* (2024) used simulations achieved in COMSOL Multiphysics to improve a new X-ray source for their stationary computed tomography (CT) design. They successfully established that the high-energy electron beam can be electronically switched "on" and "off", steered, and focused for distances from the midplane of cylindrical anode up to "120 mm" from the midplane. Steering the electron beam past this range was feasible, but the size and shape of the electron beam turned out to be distorted and enlarged, which is counter-productive for the image feature. They also stated the optimal set of factors that result in the favorite electronic focal spot size (1 mm × 7 mm) and shape at each source location for their system [32].

Finite Element Method and Mesh Generation

FEM is a numerical procedure for resolving difficulties depending on the potential magnitude of the boundary. Munro (in 1971) announced that he had determined the solution to the magnetic field complications of electron lenses, Accordingly, the lens is typically divided by meshes into many finite elements (FE) as small squares to be prepared for analysis. Usually, each square is subdivided into duple triangular shapes [33]. The potential magnitude can be calculated for all the mesh points. The possible expression of a symmetric magnetic lens can be formulated to be [34]:

$$F = \iint \frac{1}{2} \cdot \mu \cdot \left[\left(\frac{\partial V}{\partial z} \right)^2 + \left(\frac{\partial V}{\partial r} \right)^2 \right] \cdot 2 \cdot \pi \cdot r \cdot dz \cdot d\,r \quad \ldots\ldots\ldots\ldots (1)$$

where; (μ) is "The permeability at any point", V is "The scalar potential".

Equation (1) could be reduced at each mesh point numerically, so the involvement of ($\Delta\ f$) for any particular FE rendering to Equation (1) can be determined by the expression:

$$\Delta f = \frac{\pi \cdot \mu \cdot r_\circ}{4a} \left[\left(\sum_{i=1}^{3} b_i \cdot V_i \right)^2 + \left(\sum_{i=1}^{3} c_i \cdot V_i \right)^2 \right] \quad \ldots\ldots\ldots\ldots (2)$$

where; $r_\circ$ represents "The value of r at a centroid of element", a is "The area of the element", "$b_i = r_j - r_k$, $c_i = z_k - z_j$ ", V_i is "The scalar potential at each triangular mesh point".

From Equation (2), It only needs to establish the nodal relation for every mesh point. There is a need to determine magnetic vector potential A, where magnetic flux density B can be determined by:

$$B = \nabla \times A \quad \ldots\ldots\ldots\ldots\ldots\ldots\ldots\ldots\ldots\ldots (3)$$

So, the distribution of A can be computed by reducing the subsequent variational function as follows[35]:

$$F = \iiint \left(\frac{1}{2\,\mu} (\nabla \times A) \cdot (\nabla \times A) - J \cdot A \right) dV \quad \ldots\ldots\ldots\ldots\ldots\ldots (4)$$

where J represents "The current density (a definite value inside the coil windings and zero value outside the coil windings)", dV denotes "a small element of volume".

When the cylindrical coordinates are used, vector potential A consists of three components (A_z, Ar, A_θ), and when the lens is rotationally symmetric kind, the field can be specified with an element A_θ, and the functional Equation (Equation 4) will be formed as :

$$F = \iint \left\{ \frac{1}{2\,\mu} \left[\left(\frac{\partial A_\theta}{\partial z} \right)^2 + \left(\frac{\partial A_\theta}{\partial z} + \frac{A_\theta}{r} \right)^2 \right] - J_\theta A_\theta \right\} 2\,\pi\,r\ dz\ dr \quad \ldots (5)$$

When A_θ is calculated at all the mesh points, the magnetic flux distribution can be computed by drawing contours of magnitude ($\Psi = 2\,\pi\,r\,A_\theta$). The quantity of Ψ (z, r) at each point will characterize the total magnetic flux. The flux density components (B_z, B_r), in addition to total flux density B at each point of a lens can be computed as follows [36]:

DOI: https://doi.org/10.5281/zenodo.23270338

$$B_z = \frac{\partial A_\theta}{\partial r} + \frac{A_\theta}{r}\ ,\ B_r = -\frac{\partial A_\theta}{\partial z}\ ,\ B = \sqrt{B_z^2 + B_r^2} \ \ldots\ldots\ldots (6)$$

In the last Equation (6), the partial derivatives $(\frac{\partial A_\theta}{\partial z})$ and $(\frac{\partial A_\theta}{\partial r})$ can be obtained using numerical differentiation of magnitudes of A_θ at any mesh point. After computing values of *B*, curves of *B* can be drawn. The amounts of *B* are convenient in magnetic lenses designed to avoid saturation effects in magnetic material. Knowing the optical properties requires the axial flux density B(z). This is given accurately from Equation (6); in terms of A_θ (*z*, *r*); as [34]:

$$B(z) = \lim_{r\to 0}\left(\frac{\partial A_\theta}{\partial r} + \frac{A_\theta}{r}\right) = \lim_{r\to 0}\left(\frac{2A_\theta}{r}\right) \ \ldots\ldots\ldots\ldots\ldots..(7)$$

By taking the quantities of A_θ at first two off-axis mesh points in a vertical direction; This quantity of $B(z)$ can be calculated. So, By indicating the quantities A_1, A_2, and their off-axis space by r_1 & r_2 respectively, while, axial flux density can be obtained by [35]:

$$B(z) = \frac{r_1^2 A_1 - r_1^3 A_2}{r_1 r_2 (r_2^2 - r_1^2)} \ \ldots\ldots\ldots\ldots\ldots\ldots\ldots(8)$$

In 2023, Ali *et al.* observed a rise in the air gap outcomes in higher values of a focal length (f_o) and booth of spherical and aberration coefficients (C_s and C_c), respectively, while fixing an excitation parameter [37].

Saturated Magnetic Lens Analysis by First Order Finite Element Method (FOFEM)

The above explanation of magnetic lenses adopts that the magnetic materials have a constant permeability ($\mu = \mu_0\,\mu_r$), independent of flux density (*B*). In many actual magnetic lenses, magnetic saturation effects are significant. In such statuses, the nonlinearity of the magnetization curve (*B-H* curve) must be considered to predict the lens field precisely. Magnetic saturation effects are most important in objective lenses for transmission electron microscopes, where the ultimate possible axial flux density is necessary to reduce the aberrations. A key benefit of the finite element method is that it can handle magnetic materials with nonlinear *B-H* curves. To analyze a lens with magnetic saturation, the linear functional (Equation 4) is substituted by the nonlinear functional (Equation 4) to obtain:

$$F = \iiint (U - J_\theta A_\theta) 2\pi r\, dz\, dr, \text{ where, U(B)} = \int_0^B H(B)dB \ \ldots. (9)$$

The triple integration is over volume, and U is the material's magnetic energy per unit volume.

The minimization of this function produces a set of nonlinear finite element equations, which can be solved iteratively by the Newton-Raphson method [36], a standard procedure for solving a set of nonlinear algebraic equations. The lens is first analyzed to start the solution, assuming a constant permeability equivalent to the initial permeability on the magnetization curve ($\mu = \mu_i$). From this estimate, successive iterations are executed until the result approaches the final solution at which the functional (*F*) is minimized. Practically, about ten iterations are usually necessary to obtain adequate convergence. Suppose the lens is to be analyzed at several different excitations. In that case, it is suitable to linearly scale the calculated field solution from each preceding excitation to afford a starting point for iterating the solution for the following excitation. In a computer package for applying this method, the B-H data for the magnetic materials are usually identified as a set of points joined by a simple cubic curve, and lenses covering several different nonlinear magnetic materials can mostly be handled.

Magnetic Lens Analysis by Second-Order Finite Element Method (SOFEM)

Presentation of SOFEM to magnetic lenses and electrostatic lenses can handle many factors, such as magnetic circuit analysis, pole-piece analysis, and saturated lens analysis. In each status, the primary method is the same for the first-order elements; it uses second-order elements. Quadratic rather than linear surface patches cover the analysis area. The advantages of SOFEM over FOFEM are the same for magnetic lenses as they were for electrostatic lenses [34]: (1) much better accuracy is gotten for a given number of

DOI: https://doi.org/10.5281/zenodo.23270338

grid points; (2) curved pole-pieces can be controlled more accurately; and (3) more accurate field components can be taken out for direct ray-tracing.

Curvilinear quadrilateral meshes enclose the area to be analyzed, and it will be subdivided, using Coons patch interpolation, into second-order isoperimetric finite elements. The lens with a spherical pole piece is complex to determine with FOFEM accurately, but it is easily simulated with SOFEM. Moreover, if the spherical pole-piece has a small-bore diameter, the axial flux density is cut off very quickly inside the pole-piece. When FOFEM is used to calculate such sudden changes in axial flux density, overshoot and ringing are frequently observed in the computed axial flux density. Such artefacts are easily replaced with the greater accuracy of SOFEM.

An additional particular advantage of SOFEM over FOFEM, for magnetic lenses is that when the vector potential (A_θ) is used for the magnetic circuit and coil winding analysis, the layout of the mesh points is much less critical with SOFEM than with FOFEM. Although a better mesh layout could develop the FOFEM outcome, the circumstance that the mesh layout is essentially less critical with SOFEM is often an essential advantage in practice. This becomes important when repetitive axial derivatives of the axial flux density are calculated to compute higher-order aberrations.

One of the most significant advantages of SOFEM over FOFEM is the analysis of saturated magnetic lenses. In this situation, the permeability (μ) of the magnetic material is a function of flux density (B). In FOFEM, any specific element's permeability (μ) is uniform, so permeability changes in discrete jumps from element to element. This comparatively gross approximation and income is highly saturated pole tips with a high permeability gradient. Many elements are necessary to achieve an accurate simulation. In SOFEM, B and μ can also change within a second-order individual component; actually, B and μ can have different values at each of the 16 Gauss's points in one element. This permits a closer demonstration of physical reality with fewer points. The other significant advantage of SOFEM over FOFEM is its significantly improved accuracy for field component extraction and direct ray tracing. Combined magnetic and electrostatic lenses can be handled using the Newton-Lorentz equation of motion, which can be resolved numerically by standard fourth order – Runge -Kutta expression.

Axial flux density B (z) is necessary to value optical properties, and use known values: ($B = \mu_\circ H$, & $H = \nabla \Phi_m$) in free space regions, then, it can be concluded [31]:

$$B(z) = \mu_\circ \Phi'_m(z) \quad \ldots\ldots\ldots\ldots\ldots\ldots\ldots\ldots (10)$$

where; $\Phi'_m(z)$ represents "the derivative of the magnetic potential $\Phi_m(z)$ on the optical axis concerning z".

By numerical differentiation of $\Phi_m(z)$; the quantity $B(z)$ can be computed, and it can be drawn. Paraxial rays r (z) can similarly be calculated via resolving paraxial ray relation for magnetic lenses by the following expression:

$$r''(z) + \frac{e}{8mV} B^2(z) \,.\, r(z) = 0 \quad \ldots\ldots\ldots\ldots\ldots\ldots (11)$$

where (e / m) represents "The (charge/mass) ratio of the particle (absolute value)", V is "The beam voltage". The last expression (11) could be resolved mathematically by a "Fourth-order Runge-Kutta formula". When the quantity *B(z)* is calculated, its derivative *B'(z)* can also be computed using numerical differentiation.

Amer A. and Ahmad A. K., (2023) analytically derived the Gaussian optical properties and the first- and third-order isotropic and anisotropic chromatic aberrations of the Glaser electromagnetic lens. Then, they deliberated numerically for object magnetic immersion (OMI) for the first time based on two methods: differential-algebraic (DA) and electron optical aberration integrals. They found a good agreement between these two methods despite minor errors of order (10^{-7} -10^{-8}) [37].

DOI: https://doi.org/10.5281/zenodo.23270338

Analysis of Magnetic Lenses

The use of computers to design magnetic lenses to investigate their properties will be deliberated in this work, which is named "Computer-Aided Design (CAD)", frequently proceeding through the following three stages. The first stage is calculating the magnetic field from its initial boundary conditions. The second stage estimates the representative trajectories of electrons from the computed magnetic fields. The third stage is to compute image properties and aberration quantities from the computed paths [5].

Calculations of Magnetic Field

The present research work introduces an innovative program, Denoted "CMFD," for computing the axial magnetic flux density of axial rotation magnetic lenses. The input manner and the computation procedures have been built on a well-known set of Munro's packages, "M12 and M13". CMFD program improved the way of input and output data to be easy to use, and it can be modified with Microsoft Excel program or using any Text editor. Code of CMFD is built using "Visual Basic programming language". Its size on a disk equals 706 kB (723,456 bytes) without the help file.

Numerical simulators are vital in designing and optimizing the charged-particle systems or components. They enable the reduction of costs and efforts to improve the system and optimize work conditions . The purpose of CMFD program is to calculate the magnetic flux lines of a given magnetic lens geometry, where the magnetic flux lines are considered an essential indicator of the successful design of iron circuits and windings. This program provides a comprehensive view of the iron circuit's magnetic flux behaviors and weaknesses and indicates the flux leakage points.

Program Capabilities and Features

A program was developed to handle the plot of the magnetic flux lines (Equipotential lines) for rotationally symmetric and asymmetric magnetic electron lenses of coils and iron circuits of any cross-sectional shape and the pure windings of any shapes and turns. The program has an easy-to-use interface window.

Start Window

This is the first Window to deal with; see Figure (1), which contains a text box as a user guide and the text boxes for creating an input data file representing the geometry of the magnetic lens shape. The program required a knowledge of the data formation of magnetic systems according to the format described in Munro's Catalog for axially symmetric magnetic systems. Accordingly, the user must specify the numbers of the vertical and horizontal coarse meshes that align the geometrical shape of the borders of the geometrical shapes of the iron circuits and the windings. These two numbers are filled in the text box denoted "Vertical No." and "Horizontal No." respectively similarly, the user must determine the number of quadrilateral shapes generated by the previous alignment of the coarse meshes with shape borders to input it in the text box denoted "Section No.", filling out these text boxes enables the user to create the input file via the button denoted: "Create Excel Sheet", consequently, the new Window of Microsoft Office Excel sheet will appear, as shown in Figure (1), this data sheet file, also, prepared according to the format represented in Munro's Catalog for axially symmetric magnetic systems. The button is named "Data File" for opening previously prepared data files. Opening the data file will open the active working window of the CMFD program for editing the user magnetic lens design geometry, the fine mesh distribution, and the calculated magnetic flux lines.

DOI: https://doi.org/10.5281/zenodo.23270338

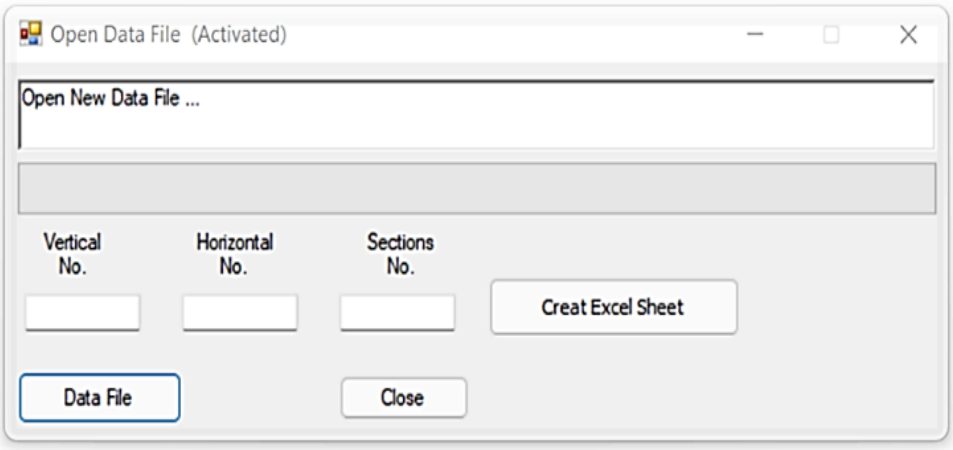


Fig. 1: Starting window of the CMFD program.

The Active Working Window of the CMFD Program

Figure (2) shows the active working window of the CMFD program, in which the user can control the editing of the flux line values, position, and distribution densities via the upper part of the Window (green dashed rectangular) and in the upper left side of the Window (black dashed rectangular), the worker can control the editing of size, colors, the position of the lens geometry, the meshes, and the flux lines. On the lower left side of the Window (blue dashed rectangle), the user can manage the data, read, export, and terminate the project. Finally, the graphics editing lies on the central part of the widow (red dashed square). The user can use a mouse and keyboard, individually or combined, to control the magnetic lens position and size.

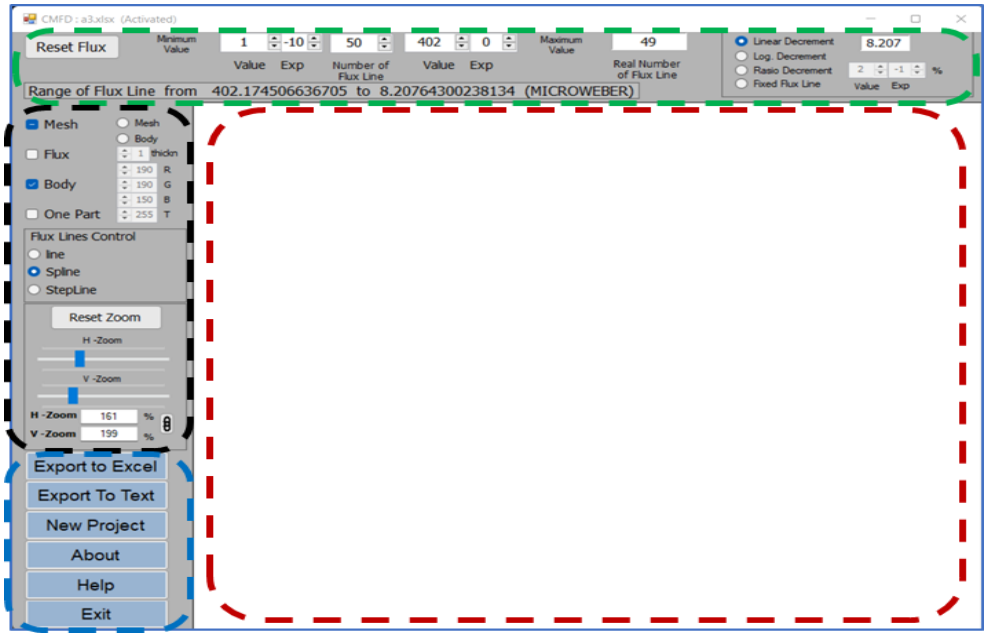


Fig. 2: The active working window of the CMFD program.

Data file

Data file format for CMFD program can be prepared in Microsoft Excel sheet Microsoft Text editor, or any compatible editor. As mentioned, the data prepared for the magnetic lens as described in Munro's catalogue describes the preparation for the magnetic lens. Figure (3) shows the prepared sample data for the proposed

DOI: https://doi.org/10.5281/zenodo.23270338

symmetrical magnetic lens. CMFD edited the lens geometry, with coarse and fine mesh distribution, for the finite element method calculations, which were created using the CMFD program input data superimposed on the lens circuit, is worth mentioning that the data prepared for the symmetrical magnetic lens, as well as the cross and fine mesh distribution, (according to Munro's method), is generated only for the one half of the upper right side of cross-section of the lens [38]. Flux line distributions are illustrated in Figure (4) below, which they calculated at a current density equal to (20.5 A/mm^2) using the default values of the program set up for the flux lines distribution and zooming, the color variation from the blue to the red represents the variation of the intensity of the magnetic field, where the red regions more significant magnetic fields than the blue one.

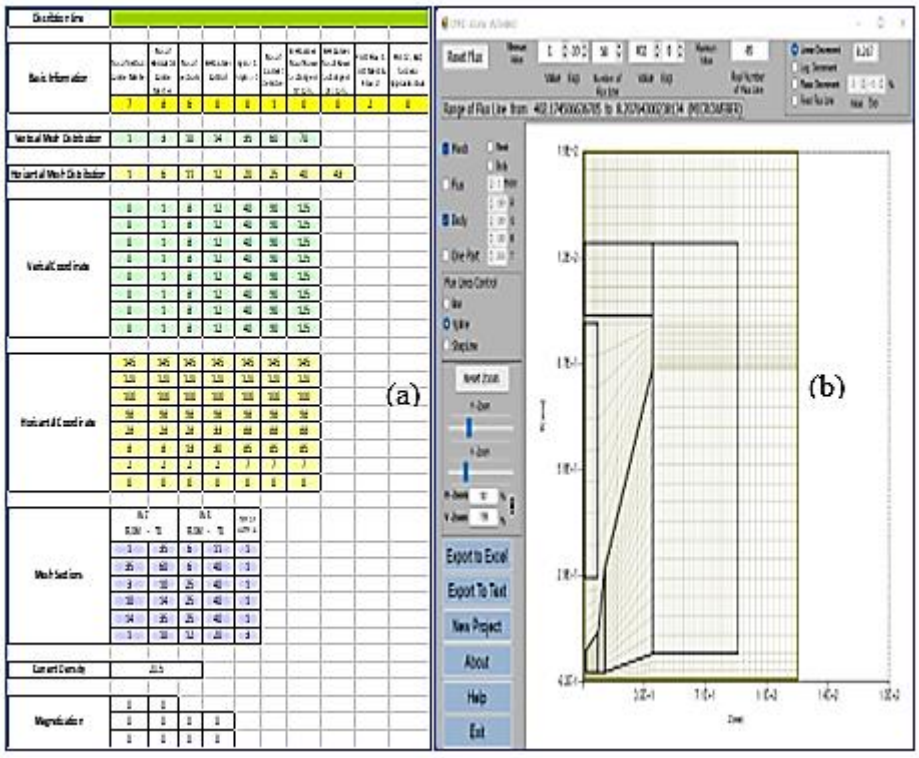


Fig. 3: (a) Microsoft Excel sheet editing of the sample data preparation. (b) CMFD editing of upper right part of cross-section of the proposed symmetrical lens and both cross and fine mesh distributions.

DOI: https://doi.org/10.5281/zenodo.23270338

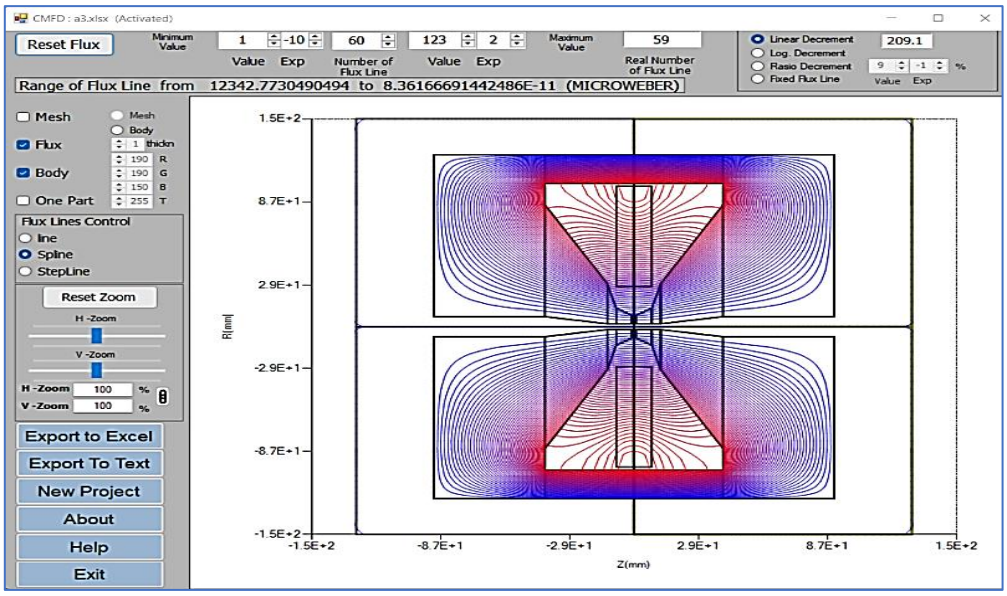


Fig. 4: The flux lines distributions calculated using CMFD program at current density of (20.5 A/mm^2) superimposed on the cross-section of the proposed magnetic symmetrical lens.

Effect of Coil Inner Radius on Flux Lines Distribution Trajectories at Pole-piece Region

This sample study demonstrates part of the program's capabilities to investigate the geometrical parameters of the magnetic systems on the flux line distributions. The study includes the variation of the inner radius of the coil, denoted (R_C), of the proposed symmetrical magnetic lens. The values of R_C are chosen equal to (14, 21, and 28 mm), and the calculations are at a constant value of the current density equal (20.5 A/mm^2). Figure (5) shows the variation of the flux line trajectories at the pole-piece region of the proposed symmetrical magnetic lens (solid black line) due to the variation of the inner radius of the energizing coil Rc, calculated using the CMFD program.

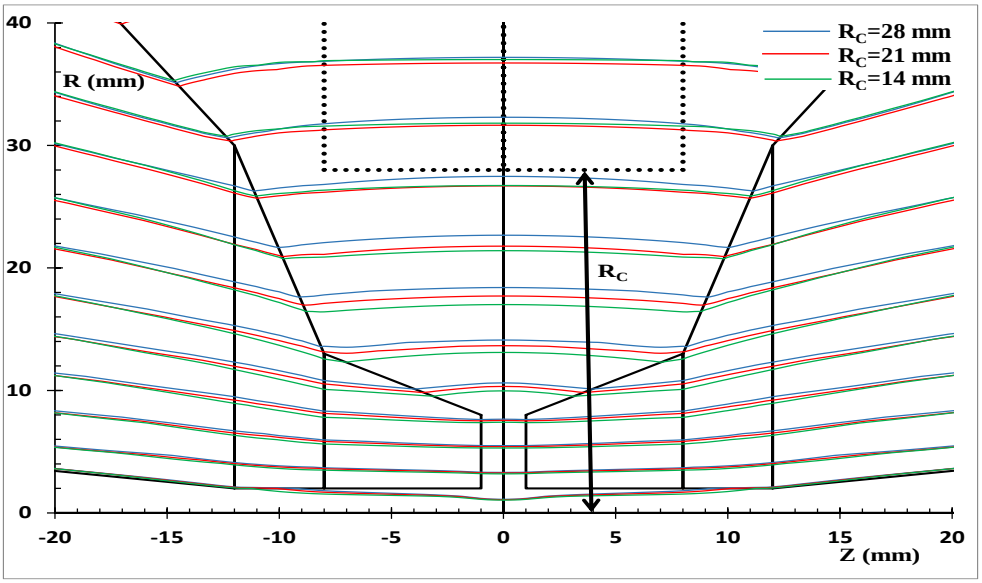


Fig. 5: Variation of the flux lines trajectories at the polepiece region.

DOI: https://doi.org/10.5281/zenodo.23270338

Conclusion

A new program has been introduced to calculate the magnetic flux line trajectories of magnetic systems, such as the magnetic electron lenses, that are excited using coil windings. The program denoted "CMFD" as an abbreviation for "Calculating Magnetic flux Density". The program possesses many features, such as the flexibility of reading the input data using any text editor, the flexibility of exporting data to Microsoft Excel or Text File Extension, the ability to plot the magnetic flux lines directly, and the system circuit furthermore, the flexibly to change both of course and the fine meshes for finite element calculations. A new suggested design of a magnetic lens has been investigated using the software written in this work to demonstrate a part of the program's capabilities to analyze the geometrical parameters of the magnetic systems on the flux line distributions. This study found that this new program is easy to use and can draw magnetic flux line trajectories with high clarity and accuracy.

Author Contributions

Researcher A provided the basic idea for the research and participated in interpreting the analytical results, gave the notices for improving the new computer program, wrote the manuscript, and analyze the outcome data. Researcher B wrote a new computer program to analyze the physical properties mentioned in the research. Researcher C compared the results of a magnetic lens studied using another internationally recognized program with the results of the new program designed in this research and also participated in analyzing the results.

Funding Statement: "Not Applicable"

Conflicts of Interest: "No competing interests"

Ethical Approval and Consent: "Not Applicable"

References

[1] Park M.-J., Kim D.H., Park K., Jang D. Y., and Han D.-Ch., "Design and fabrication of a scanning electron microscope using a finite element analysis for electron optical system", Journal of Mechanical Science and Technology,.**22**, 1734-1746, (2008). https://doi.org/10.1007/s12206-008-0317-9

[2] Bogner A., Jouneau P.-H., Thollet G., Basset D., and Gauthier C., "A history of scanning electron microscopy: Towards wet-STEM imaging, Micron", **38**,390-401, (2007). https://doi.org/10.1016/j.micron.2006.06.008

[3] Al-Azawy A. A. R., Al-Kadumi A. K. S., and Najm Z. N., "Focusing of Charged Particles Beam by Double Quadrupole Triplet Electrostatic Lenses", Journal of Kerbala University, **15**(1), 186-200, (2017). https://share.google/Fx5XN5WtaSHRpdZGS

[4] Paris G. Y., "Approximations to immersion type electrostatic lenses", Nucl. Inst. and Methods, **44**(1), 137-140, (1966). https://doi.org/10.1016/0029-554X(66)90448-4

[5] Kasper, E., "Magnetic Field Calculation and Determination of the Electron Trajectories", Magnetic Electron Lenses, ed. W. Hawkes, (Berlin, Springer), 57 – 118, (1982). https://share.google/Gfd9PR9djVbTRaoxs

[6] Lencovà B., "Software for Particle Optics Computations SPOC", Fleischnerova 15, 63500 Brno, Czech Republic, (2000). https://share.google/NhnNMRIIjbQC6UxzA

[7] Fujita Sh., Takebe M., Shimoyama H., G-Optk, "Simulation Software for Electron Gun, Characterization", 7th International Conference on Charged Particle Optics (CPO-7), Abstract for Computer Software Demonstrations, Trinity College Junior, Parlour, (2006). https://share.google/kTNICuoRbGWwyhn3M

[8] Lencovà B., Zlámal J., "Microscopy and Microanalysis", **13**(30), 2-3, (2007).

DOI: https://doi.org/10.5281/zenodo.23270338

https://share.google/H7fIRifS336wx9mo2

[9] Müller H., Uhlemann S., Hartel P., Haider M., "Aberration-corrected Optics: From an idea to a device", Proceeding of CPO-7, Eds. E. Munro and J. Rose, Physics Procedia, **1**(1), 167-178, (2008). https://share.google/NMypbNYTYYq1tV4JU

[10] Dahl D. A., "Int. J. Mass Spectrum". Vol. **200**, 3-25, (2000). https://doi.org/10.1016/S1387-3806(00)00305-5

[11] Manura D., "SIMION ® 8.0 User Manual", Scientific Instrument Service (SIS), Inc., issue 172, USA, (2008). https://share.google/rNiZLWVWIXsjir9Wn

[12] Huang T., Hu Q., Yang Z., Li B., Li J. Q., Jin X. L., Hu Y. L., Zhu X. F., Liao L., Xiao L., He G. X., "Electron Devices", IEEE Transactions on **56**(1), 140-148, (2009). https://share.google/finoHIPrHhB3z5dpX

[13] Munro E., "Munro's Electron Beam Software – Software Catalogue", MEBS Ltd, (2010). https://share.google/J94DrNTAik2KLaf81

[14] Humphries S., "Three-Dimensional Charged-Particle Optics and Gun Design", Field Precision LLC, CRC Press, Albuquerque, New Mexico U.S.A, (2011). https://share.google/5Rny2rEnz4zUB3DtS

[15] Egerton R. F., "Physical Principles of Electron Microscopy", Springer, USA, (2005). https://doi.org/10.1007/978-3-319-39877-8

[16] Szilagyi M., "Electron and Ion Optics", Plenum Press: New York, (1988). https://doi.org/10.1007/978-1-4613-0923-9

[17] Hawkes P. W., "Magnetic Electron Lenses", Springer-Verlag, Berlin, (1982). https://doi.org/10.1007/978-3-642-81516-4

[18] Liebl, H., "Applied Charged Particle Optics", Ch.1-4, Springer, pp. 1-104, (2008). https://doi.org/10.1007/978-3-540-71925-0_1

[19] Hasan H. S., "Building a new software of electromagnetic lenses (CADTEL)", International Letters of Chemistry, Physics and Astronomy, Vol. **4**, 46-55, (2013). https://share.google/gyaZqayKWdEnqmwcR

[20] Al-Obaidi H. N., and Al-Azawy A. A. R., "An Investigation Tool for Analyzing Electrostatic Lenses", Journal of College of Education, Vol. **1**, 39-64, (2016). https://share.google/gi1h7O3rJGyVYvm0N

[21] Ghani M.K.A., Mohammed M.A., Ibrahim M.S., Mostafa, S.A. And Ibrahim, D.A., "Implementing an Efficient Expert System for Services Center Management by Fuzzy Logic Controller", Journal of Theoretical & Applied Information Technology, **95**(13), (2017). https://share.google/8AKMRUZ7ULn6JD85m

[22] Ogudo, K.A., Nestor M. J., D., Khalaf O. I., Kasmaei D. H., "A Device Performance and Data Analytics Concept for Smartphones", IOT Services and Machine-Type Communication in Cellular Networks Symmetry, Vol.**11**, 593-602, (2019). https://doi.org/10.3390/sym11040593

[23] Mohammed, M.A., Ghani, M.K.A., Mostafa, S.A., and Ibrahim, D.A., "Using Scatter Search Algorithm in Implementing Examination Timetabling Problem". Journal of Engineering and Applied Sciences, Vol. **12**, 4792-4800, (2017). https://irepository.uniten.edu.my/handle/123456789/23366

[24] Kadim W. J., NASER B. A., and Abbas T. M., "Optimization of asymmetrical magnetic lenses with the aid of EOD program", International Journal of Engineering & Technology, **7**(4),3591-3594, (2018). https://share.google/UYAiH3uf2hnk3UsfK

[25] Khalaf O. I, Abdulsahib Gh. M., and Sadik M., "A Modified Algorithm for Improving Lifetime WSN". Journal of Engineering and Applied Sciences, Vol. **13**, 9277-9282, (2018). https://share.google/FKBzTKDyY2tF4Wob5

DOI: https://doi.org/10.5281/zenodo.23270338

[26] Khalaf O. I, Sabbar B. M., "An overview on wireless sensor networks and finding optimal location of node", Periodicals of Engineering and Natural Sciences, **7**(3), (2019). https://share.google/TPxaolxmJfI5SGK3V

[27] Alabdullah A. I. M., Mostafa S. A., Mohammed M. A., Mustapha A., Ramli A. A., Jubair M.A., Hassan M. H., Ismail A., Ibrahim Dh. A., "Focal Length Measurement Application for Electrostatic Immersion Lenses Approximations", REVISTA AUS, no.26-1, 199- 207, (2019). https://share.google/ozaYG79fTthrBFxqK

[28] Liu J., Fu W., Wang D., Lei Y, Huang J., Wang Y., Deng P., Cai H., "Simulation of the static spatial resolution characteristics for a dilation imager with long magnetic focusing lens", Optik - International Journal for Light and Electron Optics 204 (2020) 163506. https://doi.org/10.1016/j.ijleo.2019.163506

[29] Liu J., Fu W., Deng P.,Wang D., Huang J., Lei Y, Wang Y., Cai H., "Simulation of a pulse-dilation framing tube with sensitive diameter of 60 mm using large aperture short magnetic lens", Optik - International Journal for Light and Electron Optics 203 (2020) 163974. https://doi.org/10.1016/j.ijleo.2019.163974

[30] Khan S. A. and Jagannathan R., " Quantum mechanics of round magnetic electron lenses with Glaser and power law models of $B(z)$", Optik - International Journal for Light and Electron Optics 229 (2021) 166303. https://doi.org/10.1016/j.ijleo.2021.166303

[31] AL-Janan, M. K. A., AL-Salih, R. Y. J., "Design and study the effect of inner bore diameter on the magnetic and optical properties of the unipolar lens", Baghdad Science Journal, **20**(3),805-814, (2023). https://doi.org/10.21123/bsj.2022.7075

[32] Fox J., Lee H. K., Alajo A. B., Avachat A., "Simulation study of electron beam optics for a distributed X-ray source toward stationary CT architecture ", Nuclear Inst. and Methods in Physics Research, A 1062 (2024) 169149. https://doi.org/10.1016/j.nima.2024.169149

[33] Lencova', B., "On the use of finite element method for the computation of electron optical elements", Inst. Of Sci. Instru. Czech Academy of Sci., 147, 61264 Brno, Czechoslovakia, 813-819, (1986). https://digitalcommons.usu.edu/electron/vol1986/iss3/911

[34] Orloff J., "Handbook of Charged Particle Optics", QC372.2.D4H36, Library of Congress Cataloging-in-Publication Data, Computational Techniques for Designe of Charged Particle Systems, 13-17, (1997). https://share.google/TmVwrfTWGUzstaF7I

[35] Ali, R. SH., Hussein, M. A., and Al-Salih, R.Y.J., "Optimizing the Effectiveness of Magnetic Lenses by utilizing the Electron Optical Design (EOD) Software" Engineering, Technology & Applied Science Research, **13**(6), 11980-11984, (2023). https://doi.org/10.48084/etasr.6287

[36] Al-Salih, R.Y.J., Al-Abdulla, A.I.M., and Alkattan, E.M.A., "Simple program for computing objective optical properties of magnetic lenses", Int. J. Computer Applications in Technology, **66**(3/4), 254- 259, (2021). https://doi.org/10.1504/IJCAT.2021.120450

[37] Amer A. and Ahmad A. K., "First- and third-order chromatic aberrations in Glaser magnetic lens for object magnetic immersion", Heliyon 9 (2023) e22825. https://share.google/iU8GPtBooeAeW1GbL

[38] Ortner, M., & Bandeira, L. G. C., Magpylib: A free Python package for magnetic field computation. *SoftwareX*, *11*, 100466, (2020). https://doi.org/10.1016/j.softx.2020.100466